INTERNATIONAL JOURNAL OF ADVANCE RESEARCH, IDEAS AND INNOVATIONS IN TECHNOLOGY

ISSN: 2454-132X
Impact factor: 4.295
(Volume 4, Issue 5)
Available online at: www.ijariit.com

Artificial neural network approach for modelling of heat exchanger with different baffle segment configurations

Sanjay Sharma
sanjay7june@gmail.com
Patel College of Science and Technology, Bhopal, Madhya Pradesh

Amit Kumar
amitavit689@gmail.com
Patel College of Science and Technology, Bhopal, Madhya Pradesh

ABSTRACT

In this work, two neural networks namely Cascade Feed Forward Neural Networks (CFFNN) and Feed Forward Neural Networks (FFNN) are modelled for the prediction of shell side pressure drop and heat transfer coefficient heat exchanger from its hot water flow rate. Simulation results showed that for same shell side mass flow rate, Heat transfer coefficient, pressure drop, and heat transfer rate are found to be maximum with single segmental baffles. All the two ANN models are trained, validated and tested which predicted the shell side pressure drop and heat transfer coefficient of the Heat exchanger with acceptable accuracy and the both Neural Network is found to have the best accuracy by having the best Regression due to its feedback connections

Keywords— *Shell and tube heat exchanger, CFFNN, FFNN, Baffle segment configuration*

1. INTRODUCTION

The difficulties in heat transfer analysis by conventional methods like imperfect, uncertain and noisy experimental data, many assumptions in the analysis in terms of thermos-physical properties of fluids, tedious fundamental equations, long computation time and less accuracy, direct correlations in terms of dimensionless numbers prove to be approximate analysis. These all drawbacks are being modified by ANN modelling without knowing the physical system in detail. It is seen that ANN methodologies represent a promising tool to approach and solve difficult heat transfer problems. There are some shortcomings like the need of reliable experimental data and uncertainty in the selection of ANN parameters in modelling which can be reduced by implementation this methodology in many heat transfer applications.

From the literature review, it is observed that STHX with single segment baffles, helical baffles with different helix angles, and flower baffles were studied and compared for improving the performance. However, comparison of simulations has not been done with the same specification of STHX and input conditions with segmental baffles and flower baffles by considering variations in parameters value. Hence the novel idea is to study the effects of different configurations of baffles such as segmental baffles and flower baffles in shell and tube heat exchanger (STHX) on heat transfer coefficient and pressure drop has been carried out.

ANN model for overall heat transfer coefficient of a design heat exchanger system is developed using FFNN and CFFNN neural network and trained. The developed model is validated and tested by comparing the results with the simulation results.

2. RESEARCH METHODOLOGY

In this work, performance for shell and tube heat exchanger is developed using artificial neural networks (ANNs). Simulations are conducted based on the full factorial design of experiments to develop a model using the parameters such as temperatures and flow rates. ANN model for overall heat transfer coefficient of a design/ clean heat exchanger system is developed using FFNN and CFFNN neural network and trained. The developed model is validated and tested by comparing the results with the simulation results.

3. SPECIFICATION OF SHELL AND TUBE HEAT EXCHANGER

In this study shell and tube heat exchanger with 10 different baffles are placed along the shell in alternating orientations with cut facing up, cut facing down, etc., in order to create flow paths across tube bundle. The geometric modelling is done using CAD software called CATIA V5R21 because it is easy to model Heat exchanger in 3D modelling software.

An STHX with different baffle geometries is designed [15, 16, and 17] to study the effects of variations in baffle geometry. A water-water shell and tube heat exchanger is designed considering the data in the following table 1. Fig. 1 shows single segmental baffle respectively. Fig. 2 shows flower-A and flower-B type baffles respectively.

Table 1: Dimensions of the shell side and tube side of the heat exchanger

Specification	Dimensions
Length of the heat exchanger, L	610 mm
Shell outer diameter, DS	160 mm
Tube length, l	610 mm
Tube outer diameter, do	16 mm
No. of tubes, Nt	21
Baffle spacing, ΔBt	100 mm
Baffles thickness, t	2.5 mm
No. of baffles Nb	10

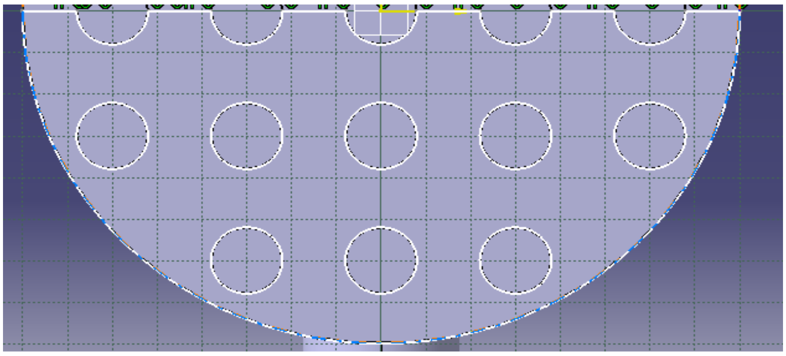

Fig. 1: Single segmental baffle

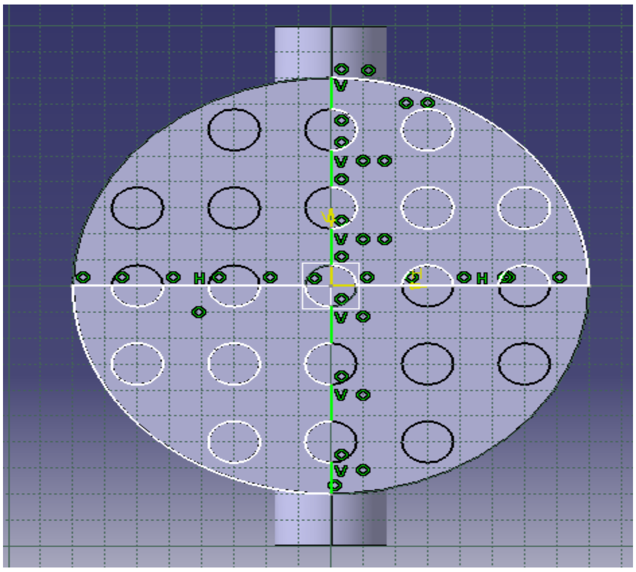

Fig. 2: Flower 'A' baffle

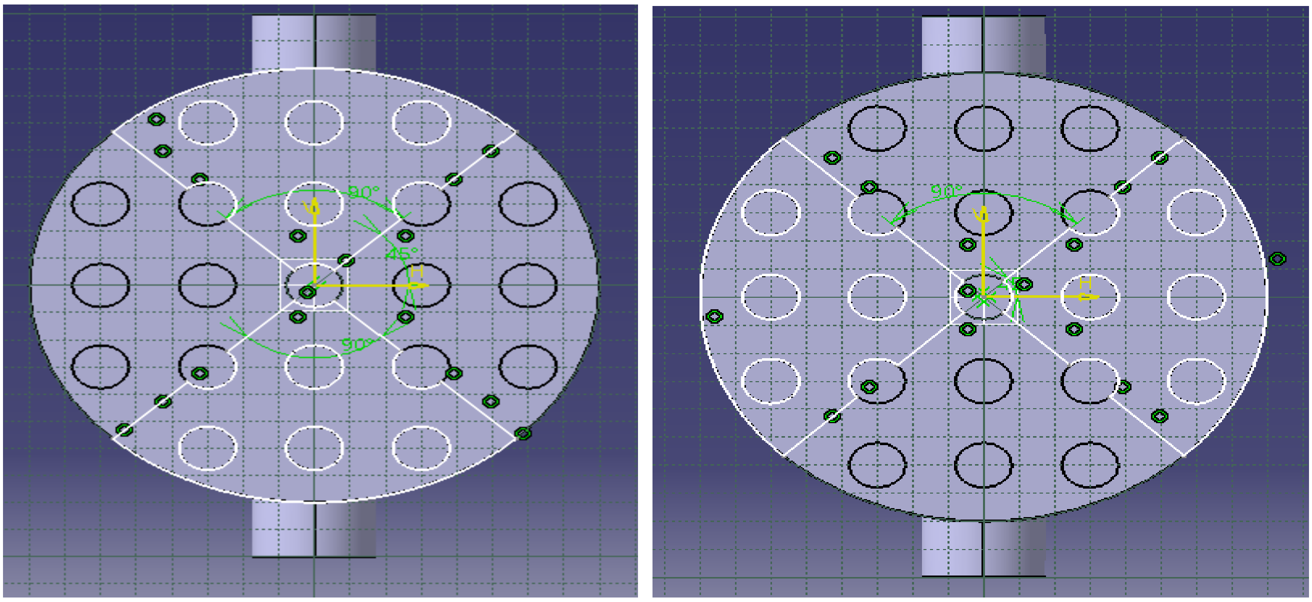

(a) **(b)**

Fig. 3: Flower 'B' baffle

4. BOUNDARY CONDITIONS

Different boundary conditions were applied to different zones. Since it is a shell-and-tube heat exchanger, there are two inlets and two outlets. The inlets were defined as velocity inlets and outlets were defined as pressure outlets. The water inlet boundary conditions are set as Flow opening inlets and outlet boundary conditions are set as Pressure opening outlets. The exterior wall is modelled as adiabatic. The simulation is solved to predict the heat transfer and fluid flow characteristics by using k-ε turbulence model.

Shell side inlet is set as flow opening the mass flow rate varied from 0.7533 kg/s for different simulations and temperature is set to 303 K.

Tube side inlet is set to flow opening the mass flow rate is varied from 0.7 kg/s to 1.2 kg/s and the temperature is set to 363 K.

5. RESULTS AND DISCUSSION

5.1 Pressure variations with different segmental baffle configurations in STHX

Pressure Distribution across the shell and tube heat exchanger is given below in figure 4. Pressures vary largely from the inlet to outlet. The contours of static pressure are shown in the entire figure to give a detailed idea.

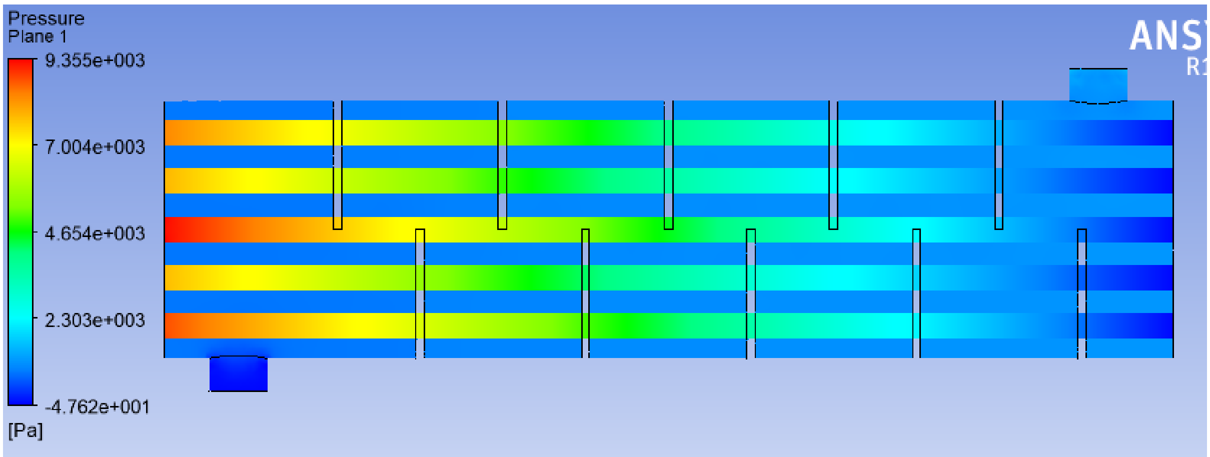

(a)

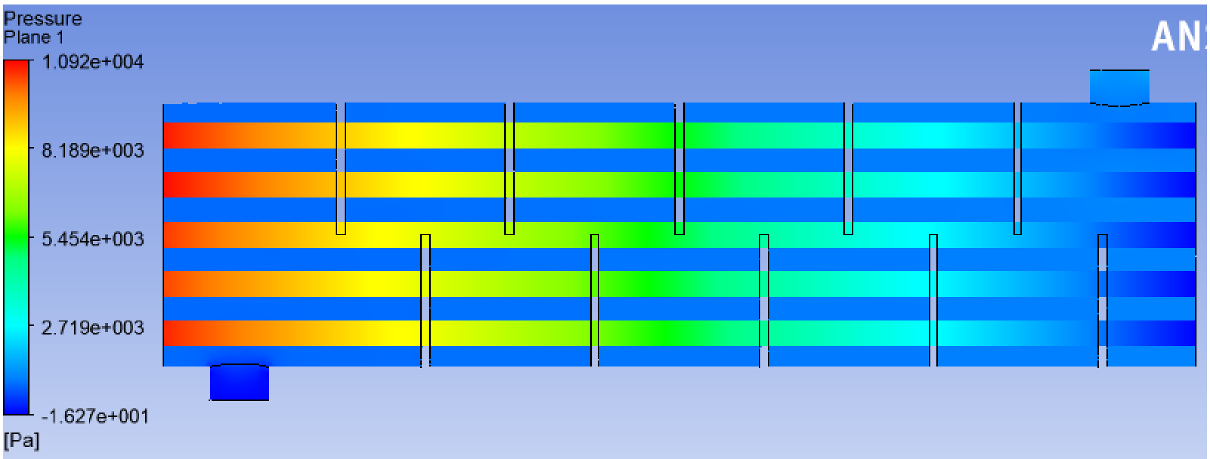

(b)

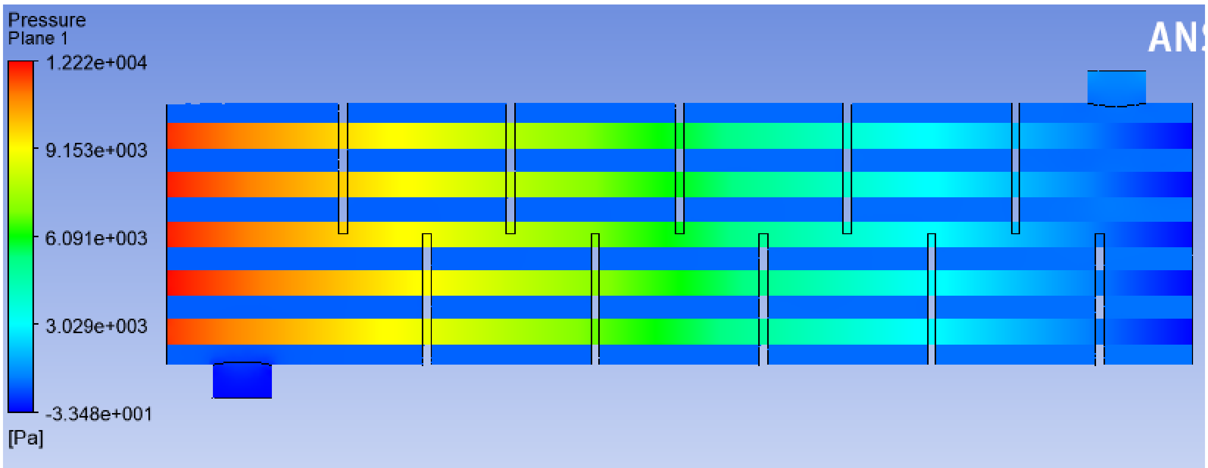

(c)

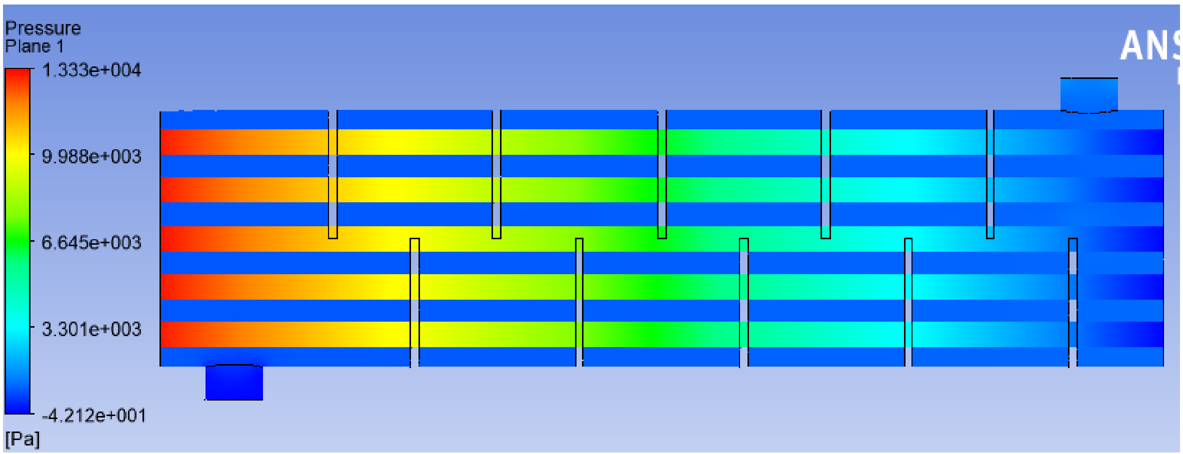

(d)

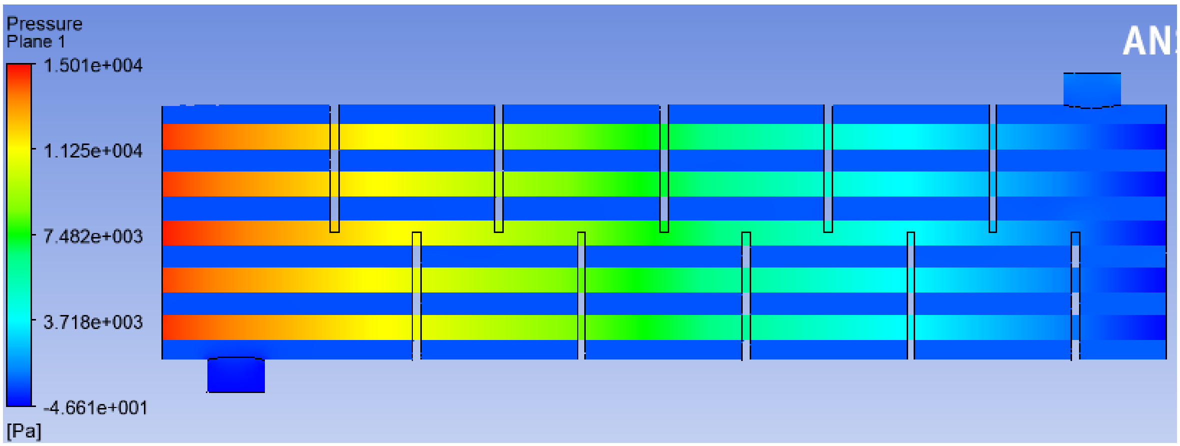

(e)

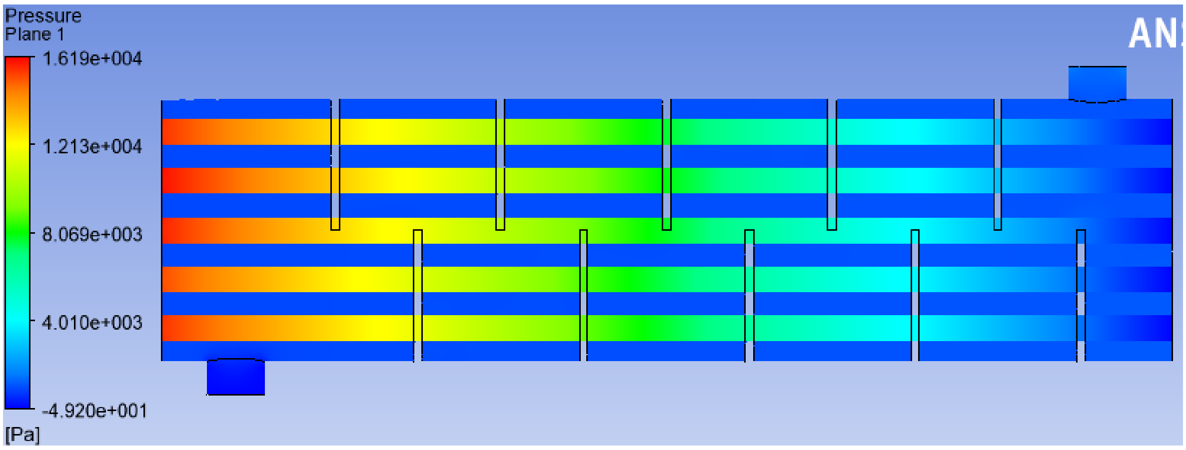

(f)

Fig. 4: Pressure variations in STHX with single segmental baffles for 6 simulations

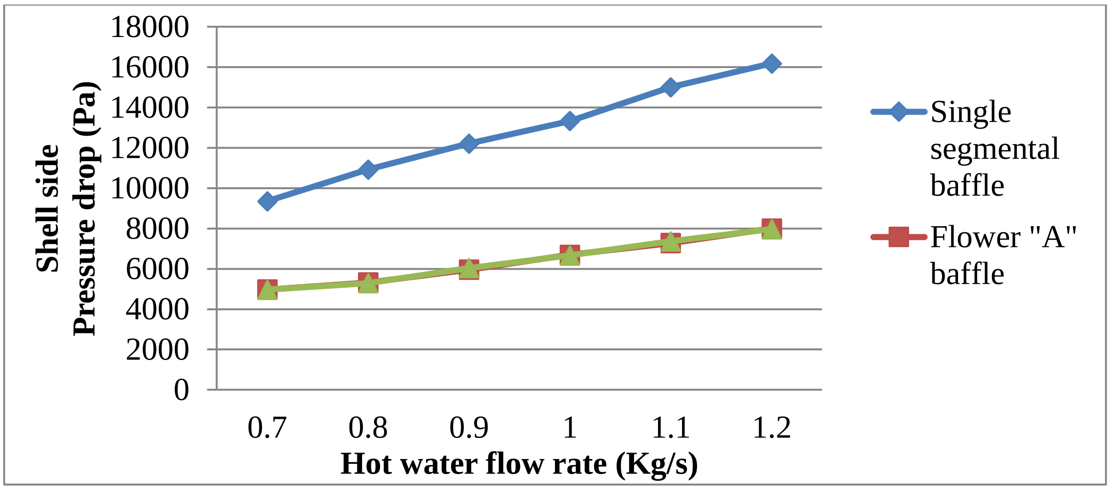

Fig. 5: Variation of shell side pressure drop in STHX with flower 'B' baffles

Hence we concluded that single segmental baffles show maximum pressure drop because of hairpin-like turns the fluid takes at the edge of the baffles. In flower 'A' or flower 'B' baffles the angle of turn of the stream lines are reduced and hence the pressure drop is minimal.

As the volumetric flow rate of the tube side fluid is increased from 0.7533 to 0.9533 Kg/s, the overall heat transfer coefficient increased from 2211 to 2470 W/(m^2 /K). This is because the increase in the volumetric flow rate increases the mass flow rate at a much faster rate than overall heat transfer coefficient or the heat energy transferred. Since the specific heat remains almost constant, tube outlet temperature should decrease to comply with the law of conservation of energy. As the flow rate of tube side fluid is increased, the tube side heat transfer coefficient increases, which in turn decreases fin effectiveness and surface effectiveness.

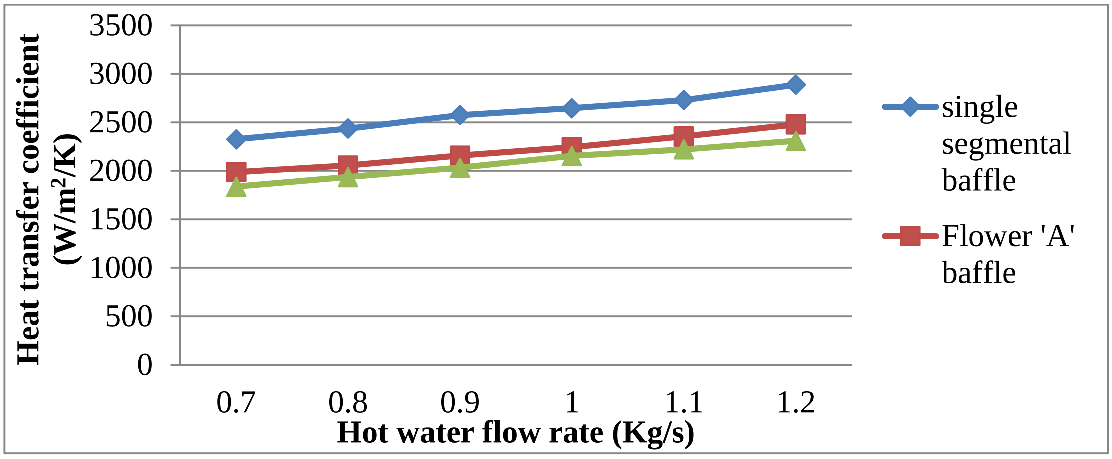

Fig. 6: Variation of heat transfer coefficient in STHX with flower 'A' baffle

Figure 6, shows the variation in the heat transfer coefficient for different baffle configurations. The slope of the curves is generally found to decrease with increase in shell side mass flow rate. Single segmental baffles show the highest heat transfer coefficient while flower 'A' and 'B' baffles show slowest heat transfer coefficient.

Hence we can say that Flower Baffles are the most effective baffles as they reduce the pressure drop by 46 % - 51 % while the heat transfer coefficient is lowered to 13 % -21 % of that produced with single segmental baffles.

6. SIMULATION RESULTS FOR THE PREDICTION OF SHELL SIDE PRESSURE DROP AND HEAT TRANSFER COEFFICIENT FOR SINGLE SEGMENTAL BAFFLE

Two Neural Networks considered for this work are modelled, trained, validated and tested for the prediction of the shell side pressure drop of a water-water heat exchanger taking its hot water flow rate as the input.

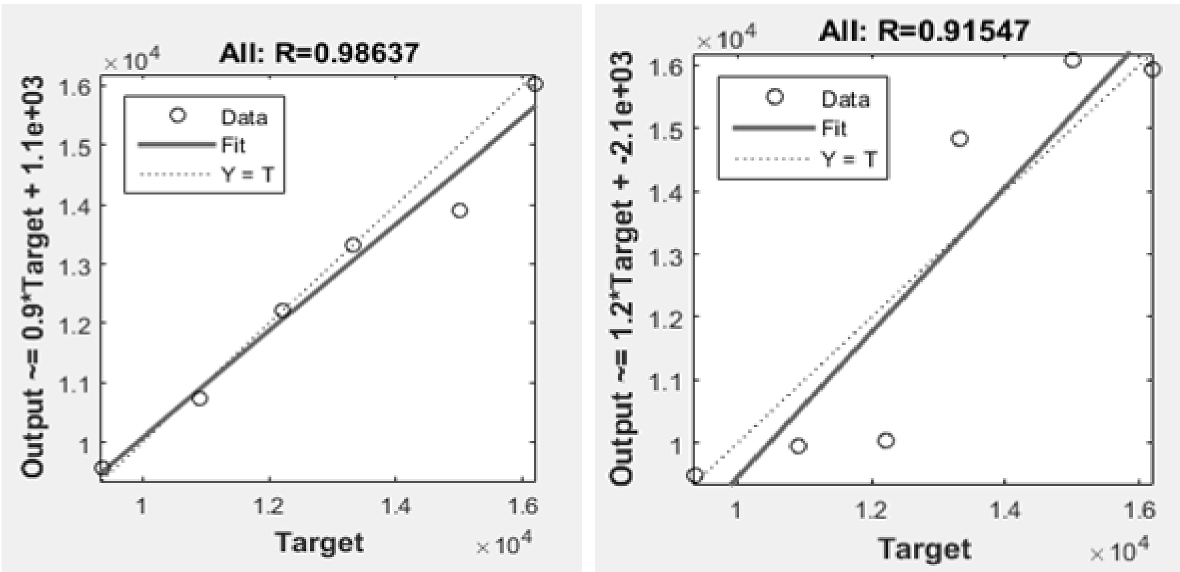

(a) FFNN **(b) CFFNN**

Fig. 7: Regression plot for shell side pressure drop in the single segmental baffle

The regression plots for FFNN and CFFNN networks are shown in figure 7. It is clear that FFNN and CFFNN Networks have been trained and can predict the shell side pressure drop in STHX with single segmental baffle. But their performance varies. The regression coefficient of FFNN is R= 0.98637 which indicates that the output variable and the input variable are better related and the output follows the input linearly. The value of R for CFFN Networks is R= 0.91547 which shows poor regression.

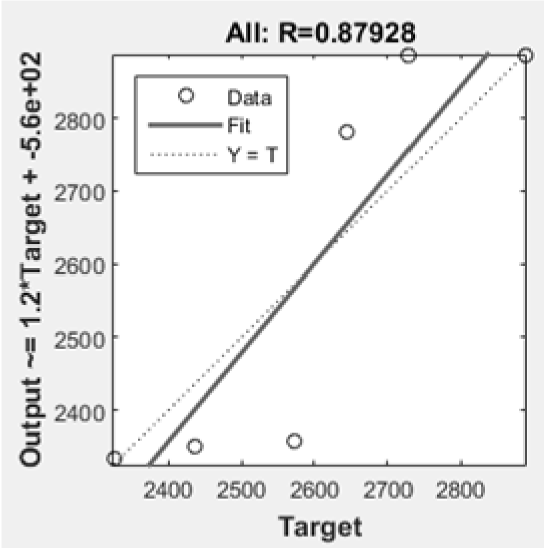

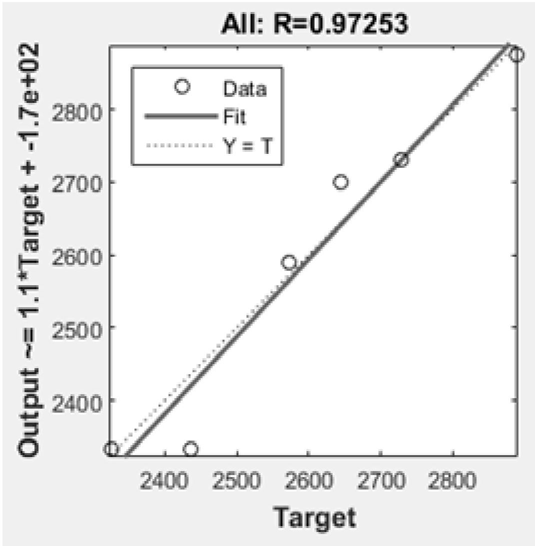

(a) FFNN **(b) CFFNN**

Fig. 8: Regression plot for the heat transfer coefficient in the single segmental baffle

The regression plots for FFNN and CFFNN networks are shown in figure 8. It is clear that FFNN and CFFNN Networks have been trained and can predict the heat transfer coefficient in STHX with single segmental baffle. But their performance varies. The regression coefficient of FFNN is R= 0.87928 which indicates poor regression. The value of R for CFFN Networks is R= 0.97253 which shows that the output variable and the input variable are better related and the output follows the input linearly.

The regression plots for FFNN and CFFNN networks are shown in figure 8. It is clear that FFNN and CFFNN Networks have been trained and can predict the shell side pressure coefficient in STHX with Flower 'A' baffle. But their performance varies. The regression coefficient of FFNN is R= 0.91788 which indicates poor regression. The value of R for CFFN Networks is R= 0.97876 which shows that the output variable and the input variable are better related and the output follows the input linearly.

7. CONCLUDING REMARKS

CFD simulation studies on Shell and Tube Heat Exchanger has been carried with single, flower 'A' type, and flower 'B' type baffle configurations. Also in this work, the performance of different neural networks namely FFNN and CFFNN for the prediction of shell side pressure drop and heat transfer coefficient of the heat exchanger are presented. The following are the conclusions arrived from these simulation studies:

1. Single Segmental Baffles provide good heat transfer coefficient but with a large pressure drop and thus consume large pumping power.
2. Flower Baffles are the most effective baffles as they reduce the pressure drop by 46 % - 51 % while the heat transfer coefficient is lowered to 13 % -21 % of that produced with single segmental baffles.
3. The slope of the curves is generally found to decrease with increase in shell side mass flow rate. Single segmental baffles show the highest heat transfer coefficient while flower 'A' and 'B' baffles show slowest heat transfer coefficient.
4. From simulation, it is inferred that the flow pattern created is similar to that created by flower 'A' baffle, except that more streamlines are observed in flower 'A' baffles when compared with flower 'B' baffles and hence lesser is the stagnation zone in flower 'A' when compared with flower 'B' baffle. Whereas in flower 'A' fluid velocity magnitude on the shell side changes periodically in the central part of the flower 'A' baffled heat exchanger. When the fluid passes a baffle, it is firstly accelerated rapidly and then flows across the breaches with large velocity. After rushing out of the breaches, the fluid is expanded suddenly and the velocity is decreased gradually. This periodic flow pattern is caused by the periodic changes of flow area which is induced by the arrangement of flower baffles. Moreover, it is also noticed that in the downstream just behind a baffle, two recirculation flow regions are generated, where the velocity magnitude is very small.
5. Single segmental baffles show maximum pressure drop because of hairpin-like turns the fluid takes at the edge of the baffles. In flower 'A' or flower 'B' baffles the angle of turn of the stream lines are reduced and hence the pressure drop is minimum.
6. Pressure variations within the STHX with single, flower 'A' and flower 'B' type baffles respectively for a flow rate of 0.3 kg/s on the shell side and 0.7533 kg/s on the tube side. It is observed that the pressure drop of increasing order is as follows: 1. Flower 'A', 2. Flower 'B', and 3. Single segmental baffle.
7. Flower 'B' Baffles are more effective than Flower 'A' Baffles as they reduce the Pressure Drop to the same extent as that of Flower 'A' baffles but with a better thermal performance associated.
8. The regression plots for FFNN and CFFNN networks for shell side pressure drop in single segmental baffle shows that FFNN and CFFNN Networks have been trained and can predict the shell side pressure drop in STHX with single segmental baffle. But their performance varies. The regression coefficient of FFNN is R= 0.98637 which indicates that the output variable and the input variable are better related and the output follows the input linearly. The value of R for CFFN Networks is R= 0.91547 which shows poor regression.
9. The regression plots for FFNN and CFFNN networks plot for heat transfer coefficient in single segmental baffle shows that FFNN and CFFNN Networks have been trained and can predict the heat transfer coefficient in STHX with single segmental baffle. But their performance varies. The regression coefficient of FFNN is R= 0.87928 which indicates poor regression. The value of R for CFFN Networks is R= 0.97253 which shows that the output variable and the input variable are better related and the output follows the input linearly.

10. The regression plots for FFNN and CFFNN networks for shell side pressure drop in flower ‘A’ baffle shows that FFNN and CFFNN Networks have been trained and can predict the shell side pressure coefficient in STHX with Flower ‘A’ baffle. But their performance varies. The regression coefficient of FFNN is R= 0.91788 which indicates poor regression. The value of R for CFFN Networks is R= 0.97876 which shows that the output variable and the input variable are better related and the output follows the input linearly.

8. REFERENCES

[1] Kute S. B., Sonage B. K (2018), “Comparison of Heat Transfer Performance of Plain Tube and Rifled Tube by Experimentation and CFD Analysis”, International Journal of Engineering Technology Science and Research, 5(1), 75-84.
[2] Shaik Himamvalli (2017), “CFD Analysis on Tube with Different Internal Fin Profiles”, International Journal of Research in Engineering and Applied Sciences, 2(3), 19-28.
[3] B. Usha Rani (2017), “Analysis of Heat Transfer through External Fins using CFD Tool”, International Journal of Modern Trends in Engineering and Research, 5(3), 81-87.
[4] K. Ravi Kumar (2017), “CFD Analysis of a Cross-flow Heat Exchanger with Different fin thickness”, International Journal of Dynamics of Fluids, 13(2), 345-362.
[5] Pankaj V. Baviskar, Kapil A. Saner, Nilesh P. Salunke, Vijay B. Jadhav (2016), “To Analyze the Effect of Varying Fin Shapes for Microprocessor Cooling”, International Journal of Innovative Research in Science, Engineering and Technology, 5(4), 5613-5621.
[6] Shobhana Singh (2016), “Parametric CFD Analysis to Study the Influence of Fin Geometry on the Performance of a Fin and Tube Heat Exchanger”, International Journal of Engineering Development and Research, 3(2), 393-399.
[7] Dibya Tripathi (2016), “Calculation of Effectiveness on the Fin Inside One Tube Plate Finned-Tube Heat Exchanger”, International Journal for Research in Applied Science & Engineering Technology, 4(11), 107-112.
[8] Poorana Chandran Karthik (2015), “Experimental and Numerical Investigation of a Louvered Fin and Elliptical Tube Compact Heat Exchanger”, Journal of Thermal Science, 19 (2), 679-692.
[9] Aditya Pratap Singh Jadaun (2015), “Thermal Analysis of Optimized Porous Fin on Various Profiles: A Review”, International Journal of Engineering Development and Research, 3(2), 393-399.
[10] Shiva Kumar (2015), “Numerical study of heat transfer in a finned double pipe heat exchanger”, World Journal of Modelling and Simulation, 11(3), 43-54.
[11] Abhishek Tripathi (2015), “A Review on Heat Transfer and Pressure Drop Correlations in Solid Circular Finned Tube Bundles Positioned at Inline and Staggered Arrangement in Cross Flow”, Internal Journal of Engineering Research and Applications, 4(12), 61-67.
[12] K. Alawadhi (2014), “Computational Fluid Dynamics (CFD) Analysis of Natural Convection of Convergent-Divergent Fins in Marine Environments”, Internal Journal of Engineering Research and Applications, 4(12), 32-36.
[13] Jignesh M. Chaudhari (2014), “Experimental Investigation of Finned Tube Heat Exchanger”, International Journal of Innovative Research in Advanced Engineering, 1(5), 67-74.
[14] Chavan D. K, Tasgaonkar G. S (2013), “CFD Analysis for Optimization of Velocity and Temperature Distribution with Modified Radiator Design at Different Fan RPM”, International Journal of Mechanical and Production Engineering Research and Development, 3(3), 9-18.
[15] Sanjay Kumar Sharma, Vikas Sharma (2013), “Maximising the Heat Transfer through Fins using CFD as a Tool”, International Journal of Recent advances in Mechanical Engineering, 2(3), 13-28.

